Climate and vegetation controls on the surface water balance: Synthesis of evapotranspiration measured across a global network of flux towers

Christopher A. Williams,[1] Markus Reichstein,[2] Nina Buchmann,[3] Dennis Baldocchi,[4] Christian Beer,[2] Christopher Schwalm,[1] Georg Wohlfahrt,[5] Natalia Hasler,[1] Christian Bernhofer,[6] Thomas Foken,[7] Dario Papale,[8] Stan Schymanski,[2] and Kevin Schaefer[9]

[1] The Budyko framework elegantly reduces the complex spatial patterns of actual evapotranspiration and runoff to a general function of two variables: mean annual precipitation (MAP) and net radiation. While the methodology has first-order skill, departures from a globally averaged curve can be significant and may be usefully attributed to additional controls such as vegetation type. This paper explores the magnitude of such departures as detected from flux tower measurements of ecosystem-scale evapotranspiration, and investigates their attribution to site characteristics (biome, seasonal rainfall distribution, and frozen precipitation). The global synthesis (based on 167 sites with 764 tower-years) shows smooth transition from water-limited to energy-limited control, broadly consistent with catchment-scale relations and explaining 62% of the across site variation in evaporative index (the fraction of MAP consumed by evapotranspiration). Climate and vegetation types act as additional controls, combining to explain an additional 13% of the variation in evaporative index. Warm temperate winter wet sites (Mediterranean) exhibit a reduced evaporative index, 9% lower than the average value expected based on dryness index, implying elevated runoff. Seasonal hydrologic surplus explains a small but significant fraction of variance in departures of evaporative index from that expected for a given dryness index. Surprisingly, grasslands on average have a higher evaporative index than forested landscapes, with 9% more annual precipitation consumed by annual evapotranspiration compared to forests. In sum, the simple framework of supply- or demand-limited evapotranspiration is supported by global FLUXNET observations but climate type and vegetation type are seen to exert sizeable additional controls.

1. Introduction

[2] One of the central challenges in the field of ecohydrology is to understand what controls the surface water balance, principally the partitioning of precipitation into evapotranspiration and runoff processes. Though land cover and climate are recognized to be important controls (along with topography, soils, etc.), observations are still needed to describe the precise nature of their controls across broad geographic domains.

[3] The typical approach to this challenge involves comparative analysis of river discharge across many catchments to infer land cover or other controls [e.g., *Choudhury*, 1999; *Donohue et al.*, 2007; *Milly*, 1994; *Peel et al.*, 2010; *Potter et al.*, 2005; *Zhang et al.*, 2001]. While revealing, attribution to drivers can remain ambiguous because of the typical heterogeneity in surface characteristics upstream of gauging stations. This paper explores a novel alternative with analysis of ecosystem-scale (order 1 km^2) evapotranspiration measurements from eddy covariance stations around the world. These FLUXNET micrometeorological stations [*Baldocchi et al.*, 2001] are located across a wide range of land cover and climate settings with well over 150 stations reporting multiyear data sets that span a diverse set of ecohydrologic conditions [*Baldocchi and Ryu*, 2011]. The combined data set offers an unprecedented opportunity to advance the hydrological sciences, witnessed by a host of

[1]Graduate School of Geography, Clark University, Worcester, Massachusetts, USA.
[2]Max Planck Institute for Biogeochemistry, Jena, Germany.
[3]ETH Zurich, Zurich, Switzerland.
[4]Environmental Science, Policy, and Management, University of California-Berkeley, Berkeley, California, USA.
[5]Institute of Ecology, University of Innsbruck, Innsbruck, Austria.
[6]Institute of Hydrology and Meteorology, Technische Universität Dresden, Dresden, Germany.
[7]Department of Micrometeorology, University of Bayreuth, Bayreuth, Germany.
[8]Department for Innovation in Biological, Agro-food and Forestry, University of Tuscia, Viterbo, Italy.
[9]National Snow and Ice Data Center, University of Colorado, Boulder, Colorado, USA.

Corresponding author: C. A. Williams, Graduate School of Geography, Clark University, 950 Main St., Worcester, MA 01610, USA. (cwilliams@clarku.edu)

recent syntheses documenting ecosystem carbon cycle sensitivity to drought [*Schwalm et al.*, 2010b; *Schwalm et al.*, 2011a; *Schwalm et al.*, 2011b], controls on evapotranspiration [*Teuling et al.*, 2009], growing supply limitation of the terrestrial water cycle in parts of the world [*Jung et al.*, 2010], ecosystem scale couplings between water and carbon dioxide exchanges [*Beer et al.*, 2007; *Beer et al.*, 2009], and testing and refining land surface models [e.g., *Schwalm et al.*, 2010a; *Wang et al.*, 2006; *Williams et al.*, 2009]. In an early flux tower synthesis of data from 27 sites, *Wilson et al.* [2002b] examined warm season data only and reported strong radiation and vapor pressure deficit controls on the Bowen ratio (ratio of sensible to latent heat fluxes) as well as sizable control by surface resistance and associated water limitation. They noted that deciduous forests and agricultural sites had the lowest surface resistances and Bowen ratios, both higher in coniferous forests as well as for sites with a summer dry, winter wet (Mediterranean type) climate [*Wilson et al.*, 2002b]. In this work we continue this line of exploration by examining what the expanded FLUXNET network of observations tells us about how climate and surface characteristics influence the terrestrial surface water balance.

[4]   To synthesize data across many sites for this purpose it becomes important to normalize observations so the effects of land cover and climate type can be isolated. For this purpose we adopt the nondimensional framework of *Budyko* [1974]. This simple and elegant framework (Figure 1) reduces climate to a radiative dryness index ($DI = E_p/P$, where E_p is potential evapotranspiration and P is precipitation) and the surface water balance to an evaporative index

($EI = E/P$, where E is evapotranspiration), where these variables are represented at a climatology time scale ($\geq$annual) by averaging across years. Importantly, the framework assumes steady state conditions as discussed in section 2.1. The two dimensionless quantities provide a nondimensional space that can aid exploration of the controls of radiation and moisture on annual evapotranspiration and runoff. Dryness index (DI) represents the ratio of demand to supply for which values exceeding one imply a water deficit at an annual time scale. Potential evapotranspiration was originally defined by net radiation (R_n) alone because of limited information available regarding additional terms relevant to evaporative demand, such as ground heat flux (G) and changes in energy storage, or additional, demand-side control from vapor pressure deficit. The evaporative index (EI) is the fraction of available water consumed by the evapotranspiration process and the residual ($1 - E/P$) can be inferred as the fraction consumed by runoff or deep drainage assuming no change in local storage. As such, the Budyko space has two fundamental upper bounds. The demand limit states that actual evapotranspiration cannot exceed potential evapotranspiration, and traces a 1:1 line corresponding to $E/E_p = 1$. The supply limit states that actual evapotranspiration cannot exceed water supply, requiring $EI \leq 1$ except where runon or phreatic water sources offer sizable contributions.

[5]   The Budyko framework has inspired powerful insights regarding climate and land cover controls of the surface water balance, primarily with analysis of catchment scale discharge records or with modeling exercises [e.g., *Choudhury*, 1999; *Donohue et al.*, 2007; *Eagleson*, 1978; *Milly*, 1994; *Potter et al.*, 2005; *Zhang et al.*, 2001]. Such analyses have documented the importance of climate seasonality and variability, vegetation type, rooting depth, plant phenology, and soil type [e.g., *Donohue et al.*, 2007; *Zhang et al.*, 2001]. For example, with dimensional analysis and the Pi theorem, *Milly* [1993] and *Porporato et al.* [2004] both showed how for steady state conditions, EI is a function of DI and surface storage capacity. Another work by *Milly* [1994] introduced a theoretical framework building on Budyko's and demonstrated how reduced soil water storage capacity, out of phase seasonality between P and E_p, and greater precipitation intensity all contribute to increased runoff. Some of the most insightful applications of this framework examine departures of EI from an expected value given DI and seek to attribute them to site-specific characteristics such as vegetation type or abundance [e.g., *Donohue et al.*, 2010; *Dooge et al.*, 1999]. With data from 1508 catchments across France, Sweden, the United States, Australia, and Great Britain, *Oudin et al.* [2008] found that land cover type explains some of the site-level departures in expected EI for a given DI. Similarly, *Donohue et al.* [2010] found that sites with a larger intra-annual range in satellite-based fractional absorption of photosynthetically active radiation (fAPAR) exhibit greater EI after accounting for both DI and a negative relationship with the phase offset between P and E_p. If such patterns lead to empirical fits with predictive skill, the Budyko framework could be improved, thus advancing a tool already valuable for land and water resource management applications such as estimation of water yield or recharge.
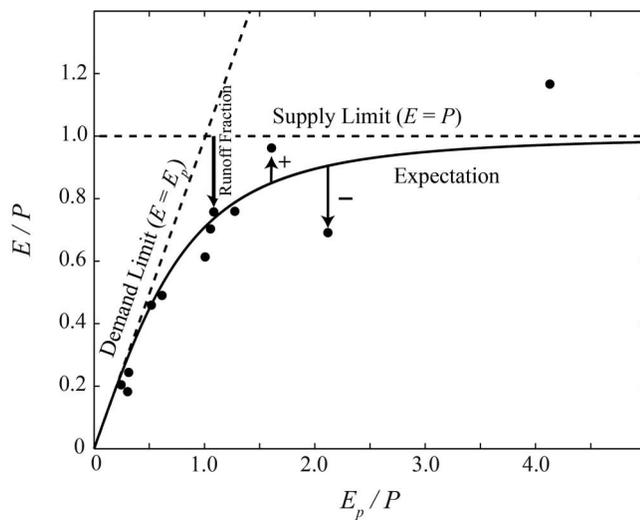

Figure 1.   Illustration of the Budyko space, composed of mean annual evaporative index (evapotranspiration/precipitation = E/P) versus mean annual dryness index (potential evapotranspiration/precipitation = E_p/P). Dashed lines indicate logical limits from demand or supply, the solid line indicates an expected value of evaporative index for a given dryness index, dots represents different sites or different years at a site, and the length of vertical arrows indicates the magnitude and sign of departure from the expected value, or the magnitude of the runoff ratio (runoff/precipitation).

[6] In this work we employ the Budyko framework, but unlike previous studies, we analyze direct measurements of evapotranspiration, and apply it at a smaller scale (of order 1 km^2) for which land cover and climate type are more clearly defined. In particular, we explore to what degree site-specific land cover and climate characteristics can explain departures from an average curve fit through data from all of the sites. Four central hypotheses are examined:

[7] Hypothesis 1: Climate types and vegetation types explain a significant fraction of variation in evaporative index after accounting for effects of dryness index. This is our most general hypothesis and offers the most comprehensive analysis spanning the full range of FLUXNET sites. It asks if vegetation or climate types act as additional controls on evaporative index, either increasing it or decreasing it relative to the expected value based on dryness index.

[8] Hypothesis 2: The evaporative index realized at a particular dryness is lower for sites with a larger seasonal hydrologic surplus (defined below, equation (2)), particularly at sites with a winter wet (Mediterranean) climate, compared to summer wet sites of the same dryness (E_p/P). Increased seasonal surplus can be expected to elevate drainage and runoff because of increased frequency of saturation overland flow and gravity drainage processes. The Mediterranean case examines a specific kind of seasonal surplus—one caused by the seasonal phase shift between rainfall and evaporative demand in winter wet climates. While this is a commonly held view and has been examined in the past, this study offers the first explicit examination of this hypothesis with a large data set of evapotranspiration at the ecosystem level.

[9] Hypothesis 3: Grasslands have a lower evaporative index (E/P) compared to forests of the same dryness index. This is expected because grasses are generally thought to have shallower root systems that lack access to the full storage of water in the vadose zone (unsaturated and saturated), and grasslands tend to have lower leaf area and associated interception capacity, and hence less direct evaporation of intercepted water.

[10] Hypothesis 4: Sites with a larger fraction of frozen precipitation have a lower evaporative index (E/P) for a given dryness index. This derives from an expectation of potentially rapid, rain-on-snow driven runoff that might elevate losses during a time of year when vegetation is less actively drawing moisture from the root zone because of cool or cold temperatures.

2. Methods

2.1. Data Treatment and Use

[11] The key observations explored in this study are evapotranspiration (E), precipitation (P), and observationally derived potential evapotranspiration [*Priestley and Taylor*, 1972]

$$E_p = \sum_{i=1}^{48} \left[\alpha Q_i \frac{\Delta_i}{\Delta_i + \gamma_i} \right] \frac{\tau}{\lambda_i}, \qquad (1)$$

where α (=1.26) is the Priestley-Taylor coefficient accounting for effects of advection and large-scale entrainment that may elevate potential evapotranspiration above

that due to radiation supply, Q is the available energy (W m^{-2} averaged for a half hour period), γ (kPa K^{-1}) is the psychrometric constant, Δ (kPa K^{-1}) is the slope of the saturation vapor pressure curve evaluated at the measured air temperature (T_a, °C), λ (=2.5 × 10^6 − 2.3668 × T_a, J kg^{-1}) is the latent heat of vaporization, and τ (=1800) is the number of seconds per half hour [*Brutsaert*, 1982; *Campbell and Norman*, 1998]. The summation in equation (1) is over 48 half hourly values in a day and thus yields a daily E_p. The analysis relies principally on the annual sum of mean daily E, P, and E_p for each site. Available energy Q is approximated in three ways: (1) with measured R_n, (2) with measured R_n minus G, and (3) from the sum of sensible and latent heat fluxes (H and λE), which effectively assumes that the lack of energy balance closure can be fully attributed to overestimation of available energy. Though the third method is not well supported by current understanding [e.g., *Foken*, 2008b], it is used here to test the robustness of findings when we force greater consistency between E_p and E. We also examine how results change when we force energy balance closure by increasing the measured turbulent fluxes to balance available energy (R_n − G) while preserving the measured Bowen ratio ($H/\lambda E$) as by *Twine et al.* [2000]. Interpretations and conclusions are unaltered by this adjustment (EP bounded; see Text S2).[1]

[12] The steady state assumption is important for use of the Budyko framework and we separate its discussion for the present application into two conditions. The first is a formal assumption that there is a negligible change in storage, here at the spatial scale of the flux tower and at the mean annual temporal scale. For nearly all of the sites used in this analysis the only water storage reservoir of consequence is field-scale soil moisture, possibly also snowpack. Of greatest relevance is the difference between soil water or snow storages at the beginning compared to the end of flux tower records and these are expected to be much smaller than annual fluxes. Canopy interception storage and changes in vegetation water content are expected to be negligible. Because data are not available to assess the magnitude of possible changes in soil or snow storages the only way to reduce their possible effects is to average data from many years of record. Flux tower records tend to be shorter than desired, with the current database having a median of 4, mean of 4.5, and range of 1 to 16 years. The second condition, somewhat related to the steady state assumption, is that net runon and net phreatic water sources are negligible, both of which could otherwise contribute additional inputs (or outputs) influencing E but not expressed in the locally measured P. These assumptions are commonly and safely adopted for catchment scale analyses, where surface runon is zero by definition and where groundwater inputs are often small and negligible, however the situation can be somewhat different for flux towers. At the flux-tower field scale, it is possible that net surface runon occurs or net subsurface lateral inputs as well, both of which could contribute to increased evapotranspiration (or conversely runoff and outputs to reduced E). Runon and subsurface flows are not measured at flux tower sites so we cannot

---

provide a quantitative examination of this issue, however both are expected to be much smaller than annual fluxes.

[13] Only trusted half hourly data are used with the remainder treated as missing. Trusted data, as defined according to the La Thuile synthesis methods, are original data or those empirically modeled with a high degree of confidence (quality control flag "fqcOK" = 1, see www.fluxdata.org for details and definition, and *Reichstein et al.* [2005, Appendix A]). We then calculate daily E, E_p, and P averaged across years but only using data when fewer than 10% of a day's half hourly data are missing. Figure 2 provides the resulting mean seasonal curve for a particular site. Only sites with gapless mean seasonal curves are analyzed, defined as those that had no more than 2 consecutive days of missing mean daily data.

[14] Of the 245 sites in the database authorized for use in this synthesis, 198 satisfied the data continuity requirements. We omit nine sites that have particularly poor energy balance closure (<0.5) defined here by the annual sum of sensible plus latent heat fluxes divided by net radiation. Four more sites are omitted due to having a ratio that exceeds reasonable bounds for the supply or demand limits. We adopt a demand limit of $E/E_p < 1.05$, retaining six sites with $1 < E/E_p < 1.05$ because of the limited precision of each estimate. We adopt a supply limit of $E/P < 1.5$, assuming that $E/P > 1.5$ is indicative of possible site-specific unit errors or data reporting problems, but also recognizing that underestimation of P or additional runon or phreatic water sources are possible particularly at the field scale of flux tower observations. Importantly, we note that adopting a stricter supply limit of $E/P < 1.05$ does not alter the interpretations or conclusions in this manuscript (ET bounded; see Text S2). Of the remaining 185 sites,
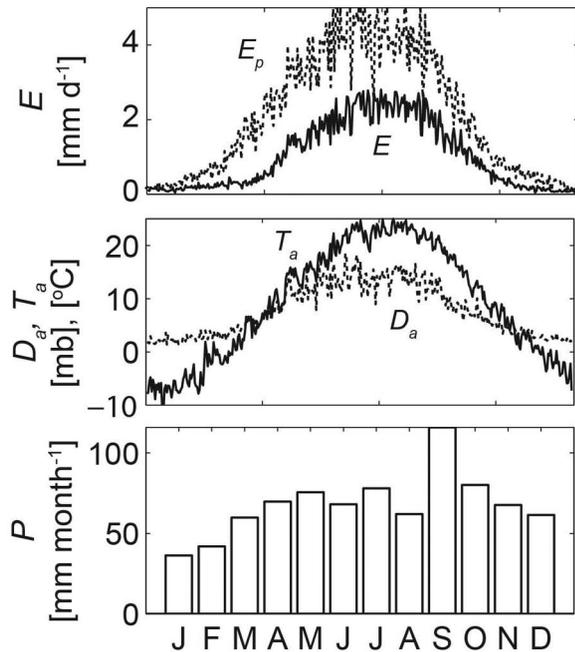
18 more are removed because of known irrigation or recent, high intensity disturbance, meaning here stand-altering fire or forest harvest, but not mowing or grazing. This leaves data from 167 sites with 764 site-years in the full analysis (see Text S1, Table S1, for site-specific details). The median record length is 4 years, the mean is 4.5 years, and the range is 1 to 16 years. Because of concerns about violation of the steady state assumption particularly for sites with short records, we examine how results change if we exclude sites with fewer than 3 years of record. Interpretations and conclusions are unaltered by this exclusion (N years filtered; Text S2).

[15] Net radiation was not reported for six sites so it is estimated as 80% of global radiation. In addition, ten sites miss one or two months of mean seasonal precipitation, which we fill based on monthly Global Precipitation Climatology Product data in the nearest 1×1 degree grid cell [*GPCC*, 2011]. These 16 sites were retained in the analysis but omitting them does not alter any of the major findings and conclusions of this paper.

[16] We obtain an approximation of the total annual precipitation arriving in a frozen form (snow, sleet, hail, graupel, etc.) at each site from the sum of precipitation in months with an average air temperature below 0°C. The climate of each site is taken from the Köppen-Geiger (K-G) climate classification [*Kottek*, 2006] and grouped as noted in Table 2. Vegetation type is classified according to the International Geosphere-Biosphere Program (IGBP) land cover type classification [*Loveland et al.*, 2001] and refined by site principal investigator reports or from review of the literature. Maximum leaf area index (L, m^2 leaf per m^2 ground) and local precipitation are obtained from the site-specific ancillary data when available in the supporting documents contributed to the La Thuile Synthesis Collection (see www.fluxdata.org).

[17] For the hydrologic surplus analyses we examine three different kinds of surpluses always relying on the climatologically averaged curves. The first is the simple annual hydrologic surplus for which we calculate annual P minus annual E_p. We also calculate the maximum accumulated monthly surplus (MAMS) at each site. For this we first calculate $P - E_p$ for each month of the climatological series. We calculate the cumulative sum of these monthly values for each month of the year and starting in any month of the year yielding a 12×12 matrix of accumulated surpluses/deficits. This can be expressed as

$$\theta_{j,k} = \sum_{k=j}^{j+11} \left[\sum_{i=j}^{k} (P_i - Ep_i) \right]_k , \qquad (2)$$

where subscript j is an index indicating the starting month (i.e., 1 = January, 2 = February, …, 12 = December), subscript k is an index indicating the number of months after the starting month ranging from 0 to 11 after j, and θ is a 12×12 matrix of accumulated monthly surpluses/deficits. We then select the maximum from the matrix $\theta_{j,k}$ and define this as a maximum accumulated monthly surplus for a particular site. This is similar to an approach applied by *Aragão et al.* [2007] in an analysis of Amazonian drought. Lastly, we introduce another surplus index that emphasizes seasonal surpluses caused by an out-of-phase arrival of

Figure 2. Example seasonal curves from one of the sites used in this analysis including evapotranspiration (E), potential evapotranspiration (E_p), air temperature (T_a), air vapor pressure deficit (D_a), and precipitation (P).

precipitation relative to losses from evaporative demand. For this we define a seasonal surplus index (SSI) by subtracting the annual hydrologic surplus (annual P minus annual E_p) from the maximum accumulated monthly surplus, with the important effect of isolating the seasonal phasing component by removing the annual total water surplus.

2.2. Analysis

[18] We solve for the best-fit curve through mean annual data for all sites to describe the mean tendency of evaporative index (E/P) as it varies with dryness (E_p/P), adopting the functional form of *Pike* [1964] because of its similarity to the original Budyko curve but with *Choudhury*'s [1999] addition of an adjustable parameter n as

$$\frac{E}{P} = \frac{1}{\left(1 + (P/E_p)^n\right)^{1/n}}. \tag{3}$$

We then calculate site-specific departures of E/P from the expected value for each site's dryness index (E_p/P) according to the fitted curve.

[19] Site departures are grouped into sample populations appropriate for evaluating each hypothesis. In general we use analysis of variance (ANOVA) to assess significance of vegetation and climate type main effects, as well as population departures from the average departure (zero) (one-sample t tests with unequal variances) or among data populations (two-sample t tests with unequal variances). For two contrasts of particular interest, forests versus grasslands and warm-temperate summer wet versus warm-temperate summer dry, we test the sensitivity of t-test results to three different methods of estimating available energy (R_n, $R_n - G$, and $H + \lambda E$). In addition, for the first two of those cases (those involving R_n), site-specific departures of E/P have a

weak linear increase with dryness index ($r^2 < 0.06$, P value < 0.01, slope ~ 0.06, intercept ~ -0.08) so we also examine how the removal of this trend influences results. Furthermore, for these particular contrasts we also examine how leaf area index and energy balance closure may differ between the populations.

[20] In our examination of potential influence from seasonal hydrologic surpluses we perform an extensive empirical model fitting exercise to assess if DI, EI, or E/P departures are a function of (a) the maximum accumulated monthly surplus, or (b) the seasonal surplus index. Using the CurveFinder function of the program CurveExpert 1.5 we examined 35 possible functional forms with two or three parameters and select the top models according to the coefficient of determination. Lastly, we perform a least squares linear regression to examine if E/P departures are a function of the fraction of precipitation that is frozen.

3. Results

[21] The synthesis data set covers a wide range of ecohydrologic settings as illustrated by the E, E_p, and P distributions shown in Figure 3. Figure 4 presents each site's location in the Budyko space (evaporative index versus dryness index) along with the best-fit curve ($n = 1.49$ with Q in equation (1) from R_n). The fitted *Choudhury* [1999] model explains more than half of the across-site variation in E/P ($r^2 = 0.62$, P value < 0.0001, standard error of 0.10). The best-fit curve has a curvature parameter $n = 1.49$, notably lower than those obtained from global syntheses of catchment-scale observations (ranging 1.8 to 2.6) by *Choudhury* [1999] and *Pike* [1964] and also lower than the value 1.9 that reproduces the original Budyko curve [*Donohue et al.*, 2011]. If we force energy balance closure by increasing the measured sensible and latent heat fluxes to

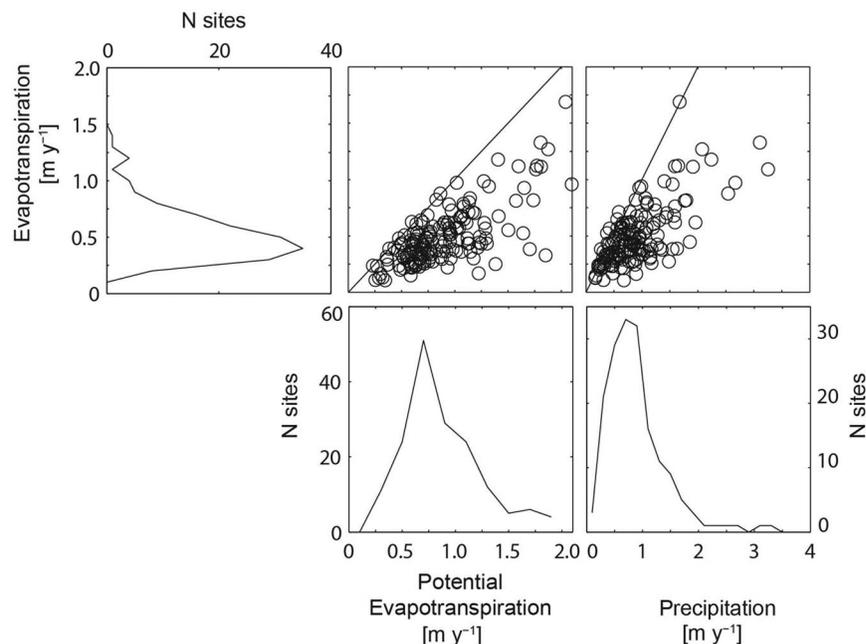

Figure 3. Scatter and frequency distributions of mean annual evapotranspiration with mean annual potential evapotranspiration or mean annual precipitation across the 167 flux tower sites analyzed in this synthesis.
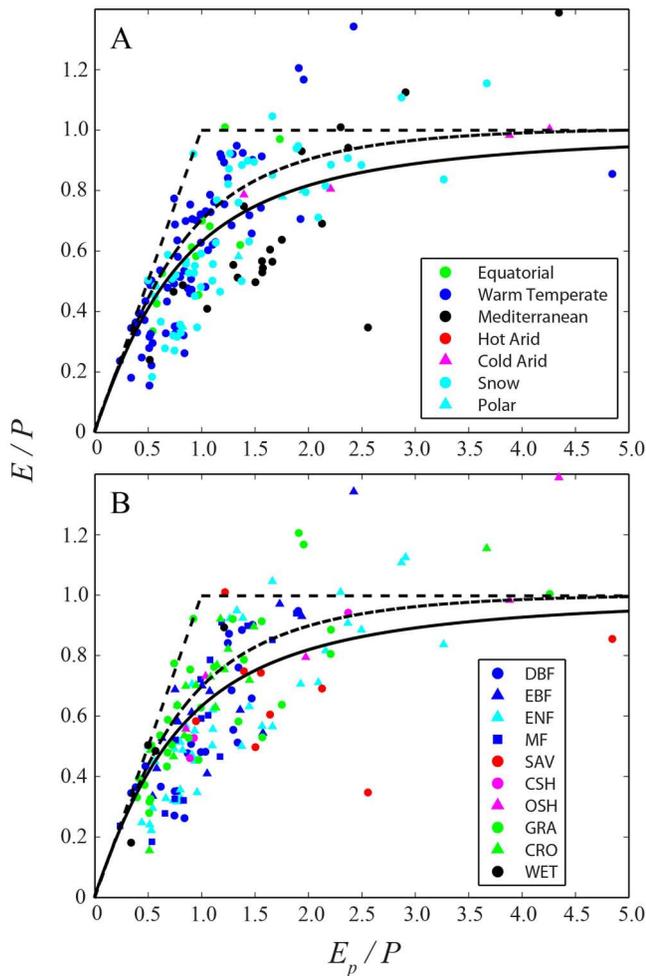
Figure 4. Evaporative index (E/P) versus dryness index (E_p/P) for all FLUXNET sites used in the analysis (one symbol for each) based on annual climatologies. Available energy for calculating E_p was estimated from net radiation. Labels correspond to (A) climate types, and (B) biome types (DBF = deciduous broadleaf, EBF = evergreen broadleaf, ENF = evergreen needleleaf, MF = mixed forest, SAV = savanna including woody savanna, CSH = closed shrubland, OSH = open shrubland, GRA = grassland, CRO = cropland, WET = wetland). Also shown are demand and supply limits (dashed straight lines), the original *Budyko* [1974] curve (dashed curve), and the best-fit curve through data for all sites (solid curve).

balance available energy while preserving the measured Bowen ratio ($H/\lambda E$), we obtain a slightly higher curvature parameter ($n = 1.58$, see Text S2), still lower than previous catchment scale studies. The relatively low curvature parameter in this work could derive from site-local climate and vegetation details, but could also indicate violation of the framework's assumptions such as that of steady state conditions and negligible contributions from water sources other than precipitation (runon or phreatic uptake). Site-specific excursions above the demand line ($E = E_p$) are negligible (i.e., <10 mm y^{-1}). However there are large excursions above the supply line ($E \leq P$) at 12 sites (of 167) for which evapotranspiration was 1.1 times precipitation

or greater (Figure 4). These particular cases might indicate that precipitation is more strongly underestimated than evapotranspiration, plausible because installation and use of gauges at FLUXNET sites do not usually follow guidelines of the World Meteorological Organization [*WMO*, 2008] and lack correction for associated wind and evaporation errors causing low bias of 5% to 20% [*Foken*, 2008a]. Correspondingly, the 1deg × 1deg Global Precipitation Climatology Project data set [*GPCC*, 2011] always recorded more precipitation than that measured at these particular FLUXNET sites (not shown). It is also possible that evapotranspiration exceeds precipitation because of lateral or upward water flows and uptake not measured with precipitation gauges (e.g., runon, subsurface hydrologic convergence, or phreatic water uptake). Since the largest deviations are limited to more arid climates ($DI > 2$), where E is typically small, they could also indicate a relatively large contribution of storage to E, i.e., the effect of violation of the steady state assumption. Nonetheless, ∼93% of the sites lie at or below the demand and supply limits, lending confidence to the use of these data for examining basic ecohydrologic hypotheses. Most importantly, the exclusion of these 12 sites from consideration in this analysis does not alter the interpretations or conclusions of this work (Text S2).

3.1. Main Effects of Climate and Vegetation

[22] We first test for significant effects of vegetation and climate on E/P departures using an analysis of variance (Table 1, two-way, unbalanced, with interaction). Both the climate and vegetation × climate interaction effects are significant (P value < 0.024) (Table 1), and the vegetation effect was nearly significant (P value = 0.088). The full model explained about 34% of the variance in E/P departures from the expectation ($r^2 = 1 -$ sum of squares for error/sum of squares total $= 1 - 2.975/4.495$), which amounts to an additional 13% of total across-site variation in E/P (=34% of the remaining 38% of unexplained variance). Thus, the combination of dryness index, vegetation type, and climate type explains 75% (=62% + 13%) of the geographic variation in climatologically averaged E/P observed at the FLUXNET sites examined in this study. This broad finding suggests that climate and vegetation type are both important determinants of E/P, supporting hypothesis 1. Thus multiple comparisons among major climate zones (Table 2) and vegetation types (Table 3) are explored next, noting still the importance of the interaction term.

Table 1. Results of a Two-Way, Unbalanced Analysis of Variance (ANOVA) Testing Effects of Vegetation, Climate and Their Interaction on Departures of E/P Relative to the Average Value Expected Based on Dryness Index, Using Q in Equation (1) From R_n, and Measured E[a]

Source	SS	df	MS	F	Prob. > F
Vegetation	0.379	10	0.0379	1.70	0.088
Climate	0.342	6	0.0570	2.55	0.023
Veg. × Clim.	0.798	18	0.0444	1.98	0.015
Error	2.975	133	0.0224		
Total	4.495	167			

[a]Veg. = vegetation; Clim. = climate; SS = sum squares; df = degrees of freedom; MS = mean squares; F = F statistic; Prob. = probability.

Table 2. Top Three Rows: Mean E/P, and Mean and SD of E/P Departures (Dep.) for Each Climate Type Where Bold, Italicized Values Have Significant Departures From Zero According to a One-Sample, One-Tailed t Test With P Value ≤ 0.05; Lowest Seven Rows: P Values From Two-Sample, Two-Tailed t Tests With Unequal Variances Between Climate Types, Where Bold Values Indicate Significance at P Value ≤ 0.05. Results Were Obtained Using Q in Equation (1) from R_n

	Warm Temp.	Medit.	Equat.	Snow	Polar	Hot Arid	Cold Arid
Mean E/P	0.59	0.66	0.63	0.65	0.63	1.19	0.90
Mean E/P Dep.	0.02	***−0.09***	0.02	−0.01	−0.09	0.24	0.04
SD E/P Dep.	0.15	0.21	0.14	0.15	0.10	0.32	0.05
N[a]	74	21	11	51	4	2	4
Warm temp.	1	**0.01**	0.90	0.28	0.17	0.05	0.75
Medit.	**0.01**	1	0.12	0.10	0.98	0.05	0.24
Equat.	0.90	0.12	1	0.47	0.15	0.11	0.80
Snow	0.28	0.10	0.47	1	0.32	**0.03**	0.48
Polar	0.17	0.98	0.15	0.32	1	0.11	0.06
Hot arid	0.05	0.05	0.11	**0.03**	0.11	1	0.24
Cold arid	0.75	0.24	0.80	0.48	0.06	0.24	1

[a]N = number of sites; Warm Temp. = warm temperate summer wet (Cw, Cf); Medit. = Mediterranean or warm temperate winter wet (Cs); Equat. = Equatorial (Af, Am, As, Aw); Snow (D); Polar (E); Hot Arid (BSh, BWh); Cold Arid (BSk, BWk). These codes in parentheses identify the corresponding Köppen-Geiger classes.

[23] Regarding climate types, Mediterranean (K-G class Cs) sites tend to have a relatively low evaporative index (E/P) compared to other climates, with significant negative departures relative to warm temperate sites in particular (Table 2). Only the Mediterranean class has significant average departure from zero (one-sided t test with unequal variance, Table 2), with E/P reduced by about 9% relative to the average across all sites. Hot arid sites have a particularly high E/P, though there are only two sites contributing to this population, one of which rests on a floodplain and also records about half as much annual precipitation compared to that reported in a 1 deg × 1 deg Global Precipitation Climatology Product [*GPCC*, 2011].

[24] Turning to vegetation's influence on the surface water balance, Table 3 shows results for multiple comparisons across IGBP cover classes. A general pattern emerges with forests (deciduous broadleaf and evergreen needleleaf) tending to have negative departures while grasslands, open shrublands, croplands, and wetlands all tend to have positive departures. Mixed forests, savannas, closed shrublands,

and evergreen broadleaf forests are intermediate, having no significant differences with other vegetation types, though we note the large spread within the savanna population in particular. Only the cropland and evergreen needleleaf types have significant average departures from zero (Table 3).

3.2. Effects of Seasonal Hydrologic Surplus and a Mediterranean Climate

[25] Hypothesis 2 anticipates lower E/P with greater seasonal hydrologic surplus after controlling for dependence on dryness index. Before inspecting seasonal surpluses, we first note relationships with the maximum accumulated monthly surplus (MAMS). Recall that this surplus reflects the annual maximum of accumulated monthly surpluses in the climatological monthly water balance $P - E_p$. Thus, even if annual E_p exceeds P, the MAMS index may exceed 0 because of the possibility of seasonal surpluses during part of the year. This index shares a fundamental negative, nonlinear relationship with dryness index (Figure 5a). Correspondingly, we find a clear negative, nonlinear

Table 3. Top Three Rows: Mean E/P, and Mean and SD of E/P Departures (Dep.) for Each Vegetation Type Where Bold, Italicized Values Have Significant Departures From Zero According to a One-Sample, One-Tailed t Test With P Value ≤ 0.05; Lowest Ten Rows: P Values From Two-Sample, Two-Tailed t Tests With Unequal Variances Between Vegetation Types, Where Bold Values Indicate Significance at P Value ≤ 0.05. Results Were Obtained Using Q in Equation (1) from R_n

	DBF	EBF	ENF	MF	SAV	CSH	OSH	GRA	CRO	WET
Mean E/P	0.57	0.65	0.61	0.55	0.79	0.64	0.87	0.64	0.69	0.51
Mean dep.	−0.05	0.03	***−0.05***	−0.02	−0.04	−0.04	0.11	***0.04***	***0.05***	0.06
Stdev dep.	0.15	0.18	0.15	0.16	0.28	0.12	0.20	0.15	0.12	0.14
N[a]	22	14	42	16	10	3	5	32	17	4
DBF	1	0.15	0.95	0.63	0.90	0.91	**0.05**	**0.04**	**0.03**	0.20
EBF	0.15	1	0.11	0.36	0.44	0.52	0.41	0.91	0.72	0.83
ENF	0.95	0.11	1	0.63	0.91	0.93	**0.04**	**0.02**	**0.02**	0.20
MF	0.63	0.36	0.63	1	0.86	0.88	0.12	0.18	0.12	0.37
SAV	0.90	0.44	0.91	0.86	1	1.00	0.29	0.25	0.24	0.53
CSH	0.91	0.52	0.93	0.88	1.00	1	0.28	0.39	0.24	0.38
OSH	**0.05**	0.41	**0.04**	0.12	0.29	0.28	1	0.33	0.41	0.63
GRA	**0.04**	0.91	**0.02**	0.18	0.25	0.39	0.33	1	0.74	0.84
CRO	**0.03**	0.72	**0.02**	0.12	0.24	0.24	0.41	0.74	1	0.98
WET	0.20	0.83	0.20	0.37	0.53	0.38	0.63	0.84	0.98	1

[a]N = number of sites; DBF = deciduous broadleaf, EBF = evergreen broadleaf, ENF = evergreen needleleaf, MF = mixed forest, SAV = savanna including woody savanna, CSH = closed shrubland, OSH = open shrubland, GRA = grassland, CRO = cropland, WET = wetland.
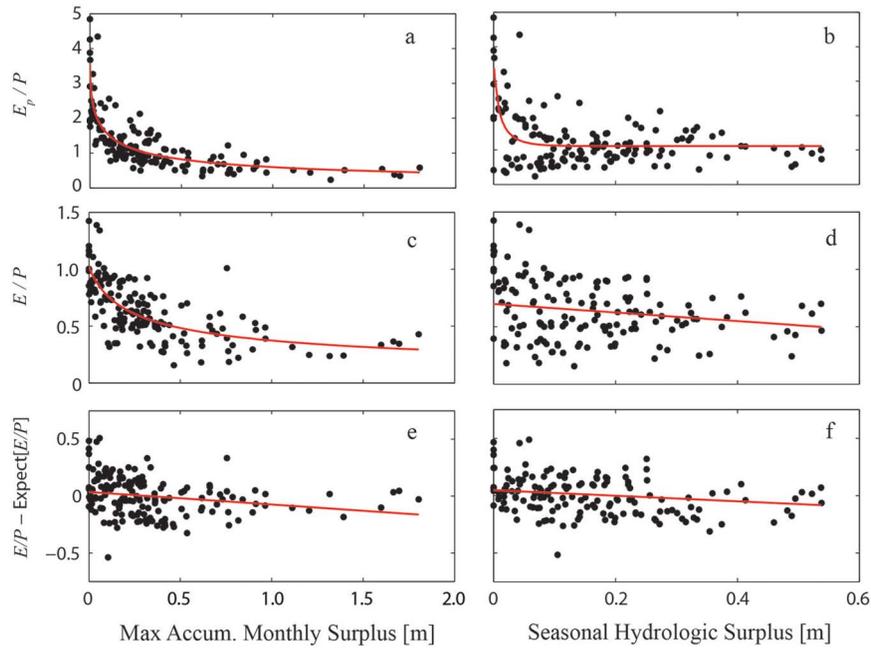
Figure 5. Relations of (a) and (b) dryness index, (c) and (d) evaporative index, and (e) and (f) departures of evaporative index relative to the expected value from the best-fit relationship to the (a), (c), and (e) maximum annual hydrologic surplus or the (b), (d), and (f) maximum seasonal hydrologic surplus. Solid lines indicate regressions for the models reported in Appendix A.

relationship between E/P and MAMS though notably with less skill compared to relationship with DI (Figure 5c, Appendix A). However, E/P departures from the mean for a given dryness index are only weakly linearly related to additional control described by the maximum accumulated monthly hydrologic surplus index (Figure 5e).

[26] To more specifically examine the possible water balance effects of seasonal surpluses we sought to isolate the seasonal component of annual surpluses with the seasonal hydrologic surplus index (SSI). The seasonal surplus index involves subtraction of the annual water balance surplus (annual P minus annual E_p) from the annual maximum of accumulated monthly surpluses described above. This seasonal surplus index is also a weak but significant determinant of E/P departures (Figure 5f, Appendix A). When collectively analyzing data from all sites, we find a weak general tendency for a decline in E/P departures with increasing seasonal surplus (-0.025% mm^{-1} H$_2$O surplus, or -14% over the range of surpluses across sites up to 575 mm). When we stratify the analysis to examine trends within climate groups, we find that this pattern is largely owing to warm temperate sites, particularly the Mediterranean class where the largest seasonal surpluses occur. For the Mediterranean-climate sites, the seasonal surplus index explains 16% of within-class variation (Table 4). Taken together, there is evidence for reduced evaporative index with greater accumulated monthly (or seasonal) hydrologic surplus, supporting hypothesis 2 and broadly consistent with the theoretical analysis of *Milly* [1994].

[27] The Mediterranean-type climate is known to have a strong seasonal hydrologic surplus owing to a seasonal phase shift between precipitation and warm-season evaporative demand. Findings above already note significant

influence on E/P, but in Table 5 we examine their robustness with statistical analysis using three different methods of estimating available energy (Q) used in calculating dryness index (methods A to C). In addition, we test sensitivity to the slight positive relationship of E/P departures with dryness index found with two of the four methods (see adjusted versus unadjusted in methods A and B).

[28] For all five approaches we find that Mediterranean sites (warm temperate winter wet climate) have lower E/P compared to warm temperate summer wet sites of the same dryness index, with approximately 11% less annual precipitation consumed by evapotranspiration on average (Table 5, P value < 0.04), supporting hypothesis 2. Mediterranean sites also tend to have a lower leaf area on

Table 4. Results From E/P Departures Linearly Regressed on the Maximum Seasonal Hydrologic Surplus by Climate Zone Reporting Number of Sites (N), Coefficient of Determination (R^2), P Value of the Regression, Slope [Departure in the % of Precipitation Consumed by Evapotranspiration mm^{-1} H$_2$O Surplus], Intercept [Departure in the % of Precipitation Consumed by Evapotranspiration], and the 90th Percentile of the Maximum Seasonal Surplus Within Each Climate Zone Population [mm H$_2$O Surplus] [a]

	N	r^2	P Value	Slope	Intercept	S90
Warm Temperate	70	0.09	0.01	-0.043	0.082	65
Mediterranean	21	0.16	0.07	-0.050	0.057	489
Equatorial	10	0.05	0.54	–	–	78
Snow	45	0.02	0.30	–	–	109
Polar	3	0.62	0.42	–	–	87

[a]Results were obtained using Q in equation (1) from R_n, and measured E. Arid sites are not shown because they lack surpluses.

Table 5. Statistics From Independent Contrasts of Site-Specific Departures ($E/P - f(E_p/P)$) (Un)adjusted for a Linear Trend of E/P Departures With E_p/P[a]

		Unadjusted			Adjusted		
	N	Mean	St. Dev.	P Value	Mean	St. Dev.	P Value
A. Q from R_n							
Mediterranean	21	−0.09	0.21	0.01	−0.12	0.19	0.00
Warm temperate	74	0.02	0.15		0.04	0.15	
Forests	48	−0.03	0.17	0.07	−0.01	0.16	0.03
Grasslands	23	0.05	0.16		0.07	0.15	
B. Q from $R_n - G$							
Mediterranean	18	−0.10	0.15	0.01	−0.13	0.12	0.00
Warm temperate	62	0.01	0.16		0.03	0.15	
Forests	41	−0.05	0.17	0.03	−0.03	0.15	0.01
Grasslands	20	0.05	0.16		0.08	0.14	
C. Q from $H + LE$							
Mediterranean	21	−0.11	0.20	0.00			
Warm temperate	72	0.02	0.12				
Forests	46	−0.03	0.13	0.05			
Grasslands	23	0.04	0.15				

[a]Contrasts are drawn between Mediterannean versus warm temperate, and forest versus grassland populations. Reported are number of sites (N), mean, and SD for sample populations, plus P values from two-sided t tests with unequal variances and using three different methods (A, B, and C) of estimating available energy for E_p.

average (Table 6, P value = 0.09), likely to be at least partly the result of rather than driver of reduced evaporative index. This finding is not due to a difference in energy balance closure (Table 7, P value > 0.40).

3.3. Grassland-Forest Contrast

[29] The somewhat surprising result of relatively high E/P in grasslands compared to forests as already noted in Table 3 would also benefit from a more restricted set of sites that removes possible interaction with climate type, as well as evaluation of this finding's robustness by using a variety of methods for calculating *DI* and *EI*. In Table 5 we report statistics for analysis including only those sites with a warm temperate climate and with a forested population that combines deciduous broadleaf, evergreen needleleaf, and mixed forest types that were found to be statistically indistinguishable (Table 3). As above, statistical analysis is presented for three methods of estimating available energy, as well as when controlling for the slight positive relationship of E/P departures with dryness index. Conclusions are consistent across these approaches as well as for additional data treatments and site exclusions explored in Text S2.

[30] Results robustly indicate that on average forests have approximately 8% less annual precipitation consumed by evapotranspiration compared to grasslands of the same

Table 6. Mean and SD of Growing Season Maximum Leaf Area Index for Climate and Vegetation Contrasts Plus P Values From Two-Sample, Two-Tailed t Tests With Unequal Variances

	Leaf Area Index		
	Mean	St. Dev.	P Value
Mediterranean	3.20	2.20	0.09
Warm temperate	4.20	2.19	
Forests	4.61	2.15	0.14
Grasslands	3.63	2.54	

Table 7. Annual Energy Balance Closure Statistics for Climate and Vegetation Contrasts Calculated With Available Energy From R_n as Well as $R_n - G$ Where Reported Plus P Values From Two-Sample, Two-Tailed t Tests With Unequal Variances

	$(H + \lambda E)/R_n$			$(H + \lambda E)/(R_n - G)$		
	Mean	St. Dev.	P Value	Mean	St. Dev.	P Value
Mediterranean	0.80	0.14	0.89	0.85	0.13	0.41
Warm Temperate	0.80	0.15		0.81	0.15	
Forests	0.80	0.15	0.23	0.80	0.15	0.13
Grasslands	0.84	0.14		0.86	0.14	

dryness index (Table 5, P value < 0.03 for five of six approaches). Pairwise comparisons (Table 3) point to deciduous broadleaf forests (DBF) and evergreen needleleaf forests (ENF) as being lower than grasslands (GRA). The difference cannot be attributed to leaf area, as forests tend to have higher not lower leaf area on average, though this is not statistically significant across the FLUXNET sites being studied (Table 6, P value = 0.14). Furthermore, energy balance closure does not differ between forested and grassland sites (Table 7, P value ≥ 0.13), agreeing with studies that report similarly good closure over a range of forest and grassland sites [*Scott*, 2010; *Wilson et al.*, 2001].

3.4. Effect of Frozen Precipitation

[31] Our last analysis examines if sites with a larger fraction of frozen precipitation have a lower evaporative index (E/P) for a given dryness owing to snowmelt runoff. A contrast between snow and warm temperate (non-Mediterranean) climates provides an indirect evaluation. Though the evaporative index in the snow compared to warm temperate climate is slightly lower on average (−3%), this difference is negligible and not statistically significant (Table 2, P value = 0.28). There is a suggestion that polar sites might have lower E/P for a given dryness compared to the warm temperate class, but again the results are not significant (Table 2, P value = 0.17).

[32] An alternative, possibly stronger method of evaluating the snowmelt runoff hypothesis is through regression of E/P departures on the fraction of annual precipitation that arrives when the surface air temperature is below freezing. We find no relationship between E/P departures and the fraction of frozen precipitation ($r^2 = 0.01$, P value = 0.28). Taken together there is no evidence that sites with a larger fraction of frozen precipitation have negative E/P departures (hypothesis 4).

4. Discussion

[33] The climate and vegetation controls reported here are broadly robust to a wide range of data treatments, with sample sizes sufficiently large (i.e., >15 sites per stratum) to detect significant differences between ecoclimatic groupings despite often wide within-sample spread. Still, it is appropriate to again discuss some of the potential limitations of the data set however unprecedented. First, precipitation and evapotranspiration are both likely undersampled because of undercatch and energy balance closure issues [e.g., *Aubinet et al.*, 2000; *Foken*, 2008a, 2008b; *Wilson et al.*, 2002a] and it is unclear by how much. Furthermore,

evapotranspirative demand is sure to deviate in space and time from the Priestley-Taylor potential (E_p) rate adopted here with a fixed α parameter [*Brutsaert*, 1982; *Hasler and Avissar*, 2007]. Nonetheless, undersampling or poor parameterization might be expected to be a random factor across sample populations (e.g., forest and grassland) and that even if they produce a systematic adjustment to the mean curve itself, the departures from the mean curve would not necessarily exhibit a strong bias for well-sampled between-population analyses.

[34] Among the major findings reported here we found that increased seasonal hydrologic surplus generally increases runoff (decreases E/P) after accounting for a site's dryness index. This is especially true for the Mediterranean climate type where the phase shift between atmospheric demand and water supply leads to elevated losses to runoff or deep drainage as inferred from low E/P. This pattern has long been established and is not surprising but it is reassuring that it is detected with direct, ecosystem-scale observations of evapotranspiration. In general this points to a limited capacity for hydrologic storage. For the Mediterranean case specifically, it indicates that storage is insufficient to fully carry over winter precipitation for summer evapotranspiration.

[35] In contrast, rejection of the snow hypothesis suggests the presence of such a carry-over, one in the form of frozen storage of winter precipitation made available only when evaporative demand is seasonally high, consistent with the pattern expected by *Milly* [1994]. Precipitation stored in the snowpack as well as frozen in cold soils becomes available to satisfy atmospheric demand when ecosystems experience increased irradiance, warm, and have elevated E_p often rising from near zero. We note that our analysis is limited by the necessity of working with a coarse approximation of frozen precipitation, estimated based on that falling in months with a mean temperature below 0°C. One could expect snowfall in some months with $T > 0$°C which also remains frozen on ground because ground $T < 0$°C as in spring, and the opposite may be true in autumn when the snow might be melted during a few days which are warm and with ground $T > 0$°C, though such effects are likely to be negligible for the annual water balance. Even so, if frozen precipitation was a strong control on EI, we would expect its signature to emerge despite the somewhat crude approximation. The absence of such control indicates that on a mean annual scale ecosystems lose a similar fraction of precipitation to evapotranspiration regardless of whether it arrives in a frozen or unfrozen form.

[36] While the above findings conform to expectations regarding climate-type controls, higher E/P in grasslands compared to forests goes against the canonical perception of many. Forests, with their higher interception [*Calder*, 1990; *Kelliher et al.*, 1993], deeper and more extensive root systems [*Jackson et al.*, 1996], and higher leaf area are generally expected to evapotranspire a larger fraction of annual precipitation. Furthermore, forest canopies have often been characterized as being better coupled to the overlying atmosphere with higher aerodynamic conductances enabling greater ventilation of canopy air and more sustained supply of dry air from the overlying atmosphere, which would tend to impose higher evaporative demand and enhance evapotranspiration rates given the same radiation and temperature conditions [*Jarvis and McNaughton*, 1986; *Jones*, 1992; *Kelliher et al.*, 1993; *McNaughton and Jarvis*, 1983]. Consistent with this canonical expectation, catchment-scale analyses show convincing evidence of reduced runoff from forested catchments compared to adjacent nonforested counterparts [*Brown et al.*, 2005; *Marc and Robinson*, 2007; *Zhang et al.*, 2001], though the difference declines as forests age [*Marc and Robinson*, 2007]. Similarly, in a global synthesis of afforested sites, *Farley et al.* [2005] reported large average reductions in annual runoff with grassland or shrubland conversion to forests (44%, 31%, respectively). And some studies measuring evapotranspiration from adjacent forest and grassland sites indicate elevated water use by forests [e.g., *Stoy et al.*, 2006].

[37] Such findings are, however, not universal. A review article by *Stednick* [1996] analyzed changes in annual water yield across paired forested and deforested catchments, indicating no detectable change in water yield for harvests smaller than 20% of catchment area, true even for some catchments that were completely deforested. In a recent example, *Wilcox and Huang* [2010] reported that woodland expansion replacing degraded grasslands caused increased, not decreased, river baseflows. In fact, wide scatter in EI for a given DI across forested catchments was reported by *Oudin et al.* [2008], showing little improvement in Budyko predictions by stratifying catchments into forest and nonforest. Across catchments of China, *Yang et al.* [2009] found that neither forest coverage nor total vegetation cover (inferred from normalized difference vegetation index) reliably explains E/P departures.

[38] Also contrary to the notion of greater water use by forests, well-established ecohydrology frameworks commonly treat grasses as having higher, not lower, transpiration rates compared to woody vegetation [*Rodriguez-Iturbe and Porporato*, 2004]. This is supported by many reports of daily mean or maximal transpiration being similar or even higher for grasses and grasslands compared to trees and forests [*Kelliher et al.*, 1993; *Larcher*, 1995; *Rodriguez-Iturbe et al.*, 2001; *Scholes and Walker*, 1993; *Scholes and Archer*, 1997; *Scholes et al.*, 2002; *Teuling et al.*, 2010; *Wolf et al.*, 2011]. It is also consistent with the idea that grasses adopt a less conservative water use strategy compared to trees [*Jones*, 1992; *Porporato et al.*, 2001; *Porporato et al.*, 2003; *Rodriguez-Iturbe et al.*, 2001]. A recent study also based on FLUXNET data showed that grasslands evapotranspire as much or more than neighboring forests, even during the early part of a heat wave when grasslands experience increased evapotranspiration along with the increased potential rate of evapotranspiration, in contrast with forests that experience increased sensible heat flux [*Teuling et al.*, 2010]. Lastly, the grasslands being studied within FLUXNET may differ markedly from those that develop after a recent forest clearing, and may instead be well adapted to their respective climate settings which may readily support and sustain grasses even if they have a shallower maximum rooting depth. Many of the forest and grassland sites under examination are in relatively mesic environments so it would be worthwhile to carefully examine if our finding extends toward regions of greater dryness where soil water limitation is more severe and deep roots

Table A1. Results of Empirical Model Fitting Between Independent and Dependent Variables for Statistically Significant Models (P Value < 0.05) With Two or Three Parameters (See Figure 5)[a]

Dependent	Independent	Model[b]	a	b	c	S.E.	r^2
Dryness index	Annual surplus	Farazdaghi-Harris	2.790E−1	1.398E0	5.722E−1	0.589	0.605
		Bleasdale	4.924E−2	3.139E0	2.439E0	0.596	0.596
		Logistic	6.181E−1	−8.087E−1	2.843E0	0.603	0.586
Evaporative index	Annual surplus	Bleasdale	9.503E−1	8.756E0	2.303E0	0.177	0.534
		Farazdghi-Harris	9.476E−1	1.764E0	6.818E-l	0.177	0.534
		Logistic	3.173E-l	−6.859E−1	1.455E0	0.177	0.534
Departure	Annual surplus	Linear	3.600E−2	−1.102E−1	–	0.162	0.056
Dryness index	Seasonal surplus	Logistic	1.104E0	−6.724E−1	3.928E1	0.783	0.323
		Bleasdale	1.506E−3	3.463E0	5.383E0	0.788	0.314
		Farazdghi-Harris	2.983E−1	1.011E0	2.937E−1	0.792	0.306
Evaporative index	Seasonal surplus	Linear	7.039E−1	−3.717E−1	–	0.254	0.047
Departure	Seasonal surplus	Linear	4.200E−2	−2.445E−1	–	0.165	0.050

[a]Functional forms were selected from examination of 35 possibilities explored with the CurveFinder function of the program CurveExpert 1.5. Those selected as top models (according to coefficient of determination r^2) are shown below, where y is the independent variable (dimensionless) and x is the dependent variable (m H_2O). S.E. refers to SE of the model.

[b]Model forms are: Linear: $y = a + bx$; Farazdghi-Harris: $y = 1/(a + bx^c)$; Bleasdale: $y = (a + bx)^{-1/c}$; logistic: $y = a/(1 + be^{-cx})$.

would become more important for maintaining high rates of evapotranspiration. Equal or higher E/P in grasslands compared to forests suggests that roots in grasslands are in fact sufficiently deep and widely spread to be capable of accessing a soil volume similar in extent to that accessed by trees, a result consistent with at least some ecosystem scale observations of rooting profiles [e.g., *Jackson et al.*, 1996; *Schenk and Jackson*, 2002; *Williams and Albertson*, 2004].

5. Conclusions

[39] Global synthesis of ecosystem-scale evapotranspiration confirms broad patterns of energy (radiative dryness) and water (precipitation) limitations, and their combined influence on the surface water balance, explaining roughly 62% of the across-site variation in evaporative index (the fraction of precipitation consumed by evapotranspiration). Climate type and vegetation type are both found to be important additional controls (+13%), modulating the first-order effects of mean annual water supply and demand. Surprisingly, forests are not found to evapotranspire a larger fraction of annual precipitation than grasslands, calling into question this common expectation.

[40] Future analyses should explore possible influences of soil characteristics, topography, and precipitation intensity, as well as seek to address measurement errors or biases in precipitation and evapotranspiration estimates or groundwater uptake as an additional water source. Because of a lack of data, this study was not able to explore possible dependence on soil physical properties despite their known influence on storage capacity and soil water retention and delivery to the soil-atmosphere, and soil-root interfaces. It would also be valuable to utilize the extensive FLUXNET database to explore how interannual relationships between evaporative index and dryness index may vary by climate type or vegetation types. Such examinations would extend this first integrative analysis across the eddy covariance network that documents support for the essential Budyko framework of surface water balance predictions, confirms sensitivity to climate seasonality and land cover type, and also challenges classical notions of water use by vegetation types.

Appendix A: Parametric Statistics for Empirical Models of Dryness or Evaporative Indexes With Surplus Indices

[41] Parametric statistics for empirical models of *DI* or *EI* with surplus indices (Table A1).

References

Aragão, L. E. O. C., Y. Malhi, M. R. Roman-Cuesta, S. Saatchi, L. O. Anderson, and Y. E. Shimabukuro (2007), Spatial patterns and fire response of recent Amazonian droughts, *Geophys. Res. Lett.*, *34*, L07701, doi:10.1029/2006GL028946.

Aubinet, M., et al. (2000), Estimates of the annual net carbon and water exchange of forests: The EUROFLUX methodology, *Adv. Ecol. Res.*, *30*, 113–175.

Baldocchi, D., and Y. Ryu (2011), A synthesis of forest evaporation fluxes—from days to years—as measured with eddy covariance, *Forest Hydrology and Biogeochemistry*, edited by D. C. M. D. E. Levia and T. Tanaka, pp. 101–116, Springer, Heidelberg.

Baldocchi, D., et al. (2001), FLUXNET: A new tool to study the temporal and spatial variability of ecosystem-scale carbon dioxide, water vapor, and energy flux densities, *Bull. Am. Meteorol. Soc.*, *82*(11), 2415–2434.

Beer, C., M. Reichstein, P. Ciais, G. D. Farquhar, and D. Papale (2007), Mean annual GPP of Europe derived from its water balance, *Geophys. Res. Lett.*, *34*, L05401, doi:10.1029/2006GL029006.

Beer, C., et al. (2009), Temporal and among-site variability of inherent water-use efficiency at the ecosystem scale, *Global Biogeochem. Cycles*, *23*, GB2018, doi:10.1029/2008GB003233.

Brown, A. E., L. Zhang, T. A. McMahon, A. W. Western, and R. A. Vertessy (2005), A review of paired catchment studies for determining

changes in water yield resulting from alterations in vegetation, *J. Hydrol.*, *301*, 28–61.

Brutsaert, W. H. (1982), *Evaporation into the Atmosphere: Theory, History, and Applications*, 299 pp., Kluwer Academic, Dordrecht.

Budyko, M. I. (1974), *Climate and Life*, Academic, New York.

Calder, I. R. (1990), *Evaporation in the Uplands*, 148 pp., John Wiley, Chichester, UK.

Campbell, G. S., and J. M. Norman (1998), *An Introduction to Environmental Biophysics*, 2nd ed., 286 pp., Springer, New York.

Choudhury, B. J. (1999), Evaluation of an empirical equation for annual evaporation using field observations and results from a biophysical model, *J. Hydrol.*, *216*, 99–110.

Donohue, R. J., M. L. Roderick, and T. R. McVicar (2007), On the importance of including vegetation dynamics in Budyko's hydrological model, *Hydrol. Earth Syst. Sci.*, *11*, 983–995.

Donohue, R. J., M. L. Roderick, and T. R. McVicar (2010), Can dynamic vegetation information improve the accuracy of Budyko's hydrological model?, *J. Hydrol.*, *390*, 23–34, doi:10.1016/j.jhydrol.2010.06.025.

Donohue, R. J., M. L. Roderick, and T. R. McVicar (2011), Assessing the differences in sensitivities of runoff to changes in climatic conditions across a large basin, *J. Hydrol.*, *406*, 234–244, doi:10.1016/j.jhydrol.2011.07.003.

Dooge, J. C. I., M. Bruen, and B. Parmentier (1999), A simple model for estimating the sensitivity of runoff to long-term changes in precipitation without a change in vegetation, *Adv. Water Resour.*, *23*(2), 153–163.

Eagleson, P. S. (1978), Climate, soil, and vegetation. 4. Expected value of annual evapotranspiration, *Water Resour. Res.*, *14*(5), 731–739.

Farley, K. A., E. G. Jobbagy, and R. B. Jackson (2005), Effects of afforestation on water yield: A global synthesis with implications for policy, *Global Change Biol.*, *11*, 1565–1576, doi:10.1111/j.1365-2486.2005.01011.x.

Foken, T. (2008a), *Micrometeorology*, 308 pp., Springer, Heidelberg.

Foken, T. (2008b), The energy balance closure problem: An overview, *Ecol. Appl.*, *18*(6), 1351–1367.

GPCC (2011), ISLSCP II Global Precipitation Climatology Centre (GPCC) Monthly Precipitation. Data set. Available online [http://daac.ornl.gov/] from Oak Ridge National Laboratory Distributed Active Archive Center, Oak Ridge, Tennessee, U.S.A., doi:10.3334/ORNLDAAC/995.

Hasler, N., and R. Avissar (2007), What controls evapotranspiration in the Amazon Basin?, *J. Hydrometeorol.*, *8*, 380–395.

Jackson, R. B., J. Canadell, J. R. Ehleringer, H. A. Mooney, O. E. Sala, and E. D. Schulze (1996), A global analysis of root distributions for terrestrial biomes, *Oecologia*, *108*(3), 389–411.

Jarvis, P. G., and K. G. McNaughton (1986), Stomatal control of transpiration: Scaling up from leaf to region, *Adv. Ecol. Res.*, *15*, 1–49.

Jones, H. G. (1992), *Plants and Microclimate: A Quantitative Approach to Environmental Plant Physiology*, 2nd ed., Cambridge University Press, Cambridge.

Jung, M., et al. (2010), A recent decline in the global land evapotranspiration trend due to limited moisture supply, *Nature*, *467*, 951–954, doi:10.1038/nature09396.

Kelliher, F. M., R. Leuning, and E. D. Schulze (1993), Evaporation and canopy characteristics of coniferous forests and grasslands, *Oecologia*, *95*, 153–163.

Kottek, M., J. Grieser, C. Beck, B. Rudolf, and F. Rubel (2006), World map of the Köppen–Geiger climate classification updated, *Meteorol. Z.*, *15*, 259–263, doi:10.1127/0941-2948/2006/0130.

Larcher, W. (1995), *Physiological Plant Ecology*, 3rd ed., 506 pp., Springer, New York.

Loveland, T., B. Reed, J. Brown, D. Ohlen, J. Zhu, L. Yang, and J. Merchant (2001), Development of a global land cover characteristics database and IGBP DISCover from 1-km AVHRR data, *Int. J. Remote Sensing*, *20*, 1303–1330.

Marc, V., and M. Robinson (2007), The long-term water balance (1972–2004) of upland forestry and grassland at Plynlimon, mid-Wales, *Hydrol. Earth Syst. Sci.*, *11*(1), 44–60.

McNaughton, K. G., and P. G. Jarvis (1983), Predicting the effects of vegetation changes on transpiration and evaporation, in *Water Deficits and Plant Growth, Vol. VII, Additional Woody Crop Plants*, edited by T. T. Kozlowski, pp. 1–47, Academic, San Diego, CA.

Milly, P. C. D. (1993), An analytic solution of the stochastic storage problem applicable to soil water, *Water Resour. Res.*, *29*(11), 3755–3758.

Milly, P. C. D. (1994), Climate, soil water storage, and the average annual water balance, *Water Resour. Res.*, *30*, 2143–2156.

Oudin, Y., V. Andréassian, J. Lerat, and C. Michel (2008), Has land cover a significant impact on mean annual streamflow? An international assessment using 1508 catchments, *J. Hydrol.*, *357*, 303–316.

Peel, M. C., T. A. McMahon, and B. L. Finlayson (2010), Vegetation impact on mean annual evapotranspiration at a global catchment scale, *Water Resour. Res.*, *46*, W09508, doi:10.1029/2009WR008233.

Pike, J. G. (1964), The estimation of annual run-off from meteorological data in a tropical climate, *J. Hydrol.*, *2*, 116–123.

Porporato, A., F. Laio, L. Ridolfi, and I. Rodriguez-Iturbe (2001), Plants in water-controlled ecosystems: Active role in hydrologic processes and response to water stress—III. Vegetation water stress, *Adv. Water Resour.*, *24*(7), 725–744.

Porporato, A., F. Laio, L. Ridolfi, K. K. Caylor, and I. Rodriguez-Iturbe (2003), Soil moisture and plant stress dynamics along the Kalahari precipitation gradient, *J. Geophys. Res.*, *108*(D3), 4127, doi:10.1029/2002JD002448.

Porporato, A., E. Daly, and I. Rodriguez-Iturbe (2004), Soil water balance and ecosystem response to. Clim. Change, *Am. Naturalist*, *164*(5), 625–632.

Potter, N. J., L. Zhang, P. C. D. Milly, T. A. McMahon, and A. J. Jakeman (2005), Effects of rainfall seasonality and soil moisture capacity on mean annual water balance for Australian catchments, *Water Resour. Res.*, *41*, W02502, doi:10.1029/2003WR002710.

Priestley, C. H. B., and R. J. Taylor (1972), On the assessment of surface heat flux and evaporation using large-scale parameters, *Mon. Weather Rev.*, *100*(2), 81–92.

Reichstein, M., et al. (2005), On the separation of net ecosystem exchange into assimilation and ecosystem respiration: Review and improved algorithm, *Global Change Biol.*, *11*, 1–16, doi:10.111/j.1365-2486.2005.001002.x.

Rodriguez-Iturbe, I., and A. Porporato (2004), *Ecohydrology of Water Controlled Ecosystems: Soil Moisture and Plant Dynamics*, Cambridge University Press, Cambridge.

Rodriguez-Iturbe, I., A. Porporato, F. Laio, and L. Ridolfi (2001), Intensive or extensive use of soil moisture: Plant strategies to cope with stochastic water availability, *Geophys. Res. Lett.*, *28*(23), 4495–4497.

Schenk, H. J., and R. B. Jackson (2002), Rooting depths, lateral root spreads and below-ground/above-ground allometries of plants in water-limited ecosystems, *J. Ecol.*, *90*(3), 480–494.

Scholes, R. J., and S. R. Archer (1997), Tree-grass interactions in savannas, *Annu. Rev. Ecol. Syst.*, *28*, 517–544.

Scholes, R. J., and B. H. Walker (1993), *An African Savanna: Synthesis of the Nylsvley Study*, Cambridge University Press, New York.

Scholes, R. J., P. R. Dowty, K. Caylor, D. A. B. Parsons, P. G. H. Frost, and H. H. Shugart (2002), Trends in savanna structure and composition along an aridity gradient in the Kalahari, *J. Veg. Sci.*, *13*(3), 419–428.

Schwalm, C. R., et al. (2010a), A model-data intercomparison of CO_2 exchange across North America: Results from the North American Carbon Program site synthesis, *J. Geophys. Res.*, *115*, G00H05, doi:10.1029/2009JG001229.

Schwalm, C. R., et al. (2010b), Assimilation exceeds respiration sensitivity to drought: A FLUXNET synthesis, *Global Change*, *16*(2), 657–670, doi:10.1111/j.1365-2486.2009.01991.x.

Schwalm, C. R., C. A. Williams, and K. Schaefer (2011a), Carbon consequences of global hydrologic change, 1948–2009, *J. Geophys. Res.*, *116*, G03042, doi:10.1029/2011JG001674.

Schwalm, C. R., C. A. Williams, K. Schaefer, I. Baker, G. J. Collatz, and C. Roedenbeck (2011b), Does terrestrial drought explain global CO_2 flux anomalies induced by El Nino? *Biogeosciences*, *8*, 2493–2506, doi:10.5194/bg-8-2493-2011.

Scott, R. (2010), Using watershed water balance to evaluate the accuracy of eddy covariance evaporation measurements for three semiarid ecosystems, *Agr. For. Meteorol.*, *150*, 219–225, doi:10.1016/j.agrformet.2009.11.002.

Stednick, J. D. (1996), Monitoring the effects of timber harvest on annual water yield, *J. Hydrol.*, *176*(1–4), 79–95.

Stoy, P. C., G. G. Katul, J. Y. Juang, K. A. Novick, H. R. McCarthy, A. C. Oishi, J. M. Uebelherr, H. S. Kim, and R. Oren (2006), Separating the effects of climate and vegetation on evapotranspiration along a successional chronosequence in the southeastern US, *Global Change Biol.*, *12*, 2115–2135.

Teuling, A. J., et al. (2009), A regional perspective on trends in continental evaporation, *Geophys. Res. Lett.*, *36*, L02404, doi:10.1029/2008GL036584.

Teuling, A. J., et al. (2010), Contrasting response of European forest and grassland energy exchange to heatwaves, *Nat. Geosci.*, *3*(10), 722–727, doi:10.1038/ngeo950.

Twine, T. E., W. P. Kustas, J. M. Norman, D. R. Cook, P. R. Houser, T. P. Meyers, J. H. Prueger, P. J. Starks, and M. L. Wesely (2000), Correcting

eddy-covariance flux underestimates over a grassland, *Agr. For. Meteorol.*, *103*, 279–300.

Wang, Y. P., D. Baldocchi, R. Leuning, E. Falge, and T. Vesala (2006), Estimating parameters in a land-surface model by applying nonlinear inversion to eddy covariance flux measurements from eight FLUXNET sites, *Global Change Biol.*, *13*, 652–670, doi:10.1111/j.1365-2486.2006.01225.x.

Wilcox, B. P., and Y. Huang (2010), Woody plant encroachment paradox: Rivers rebound as degraded grasslands convert to woodlands, *Geophys. Res. Lett.*, *37*, L07402, doi:10.1029/2009GL041929.

Williams, C. A., and J. D. Albertson (2004), Soil moisture controls on canopy-scale water and carbon fluxes in an African savanna, *Water Resour. Res.*, *40*, W09302, doi:10.1029/2004WR003208.

Williams, M., et al. (2009), Improving land surface models with FLUXNET data, *Biogeosciences*, *6*, 1341–1359, doi:10.5194/bg-6-1341-2009.

Wilson, K. B., P. J. Hanson, P. J. Mulholland, D. D. Baldocchi, and S. D. Wullschleger (2001), A comparison of methods for determining forest evapotranspiration and its components: sap-flow, soil water budget, eddy covariance and catchment water balance, *Agr. For. Meteorol.*, *106*, 153–168.

Wilson, K. B., et al. (2002a), Energy balance closure at FLUXNET sites, *Agr. For. Meteorol.*, *113*, 223–243.

Wilson, K. B., et al. (2002b), Energy partitioning between latent and sensible heat flux during the warm season at FLUXNET sites, *Water Resour. Res.*, *38*(12), 1294, doi:10.1029/2001WR000989.

Wolf, S., W. Eugser, S. Majorek, and N. Buchmann (2011), Afforestation of tropical pasture only marginally affects ecosystem-scale evapotranspiration, *Ecosystems*, *14*, 1264–1275, doi:10.1007/s10021-011-9478-y.

World Meteorological Organization (2008), Guide to meteorological instruments and methods of observation, *WMO No. 8*, 7th ed., WMO, Geneva, Switzerland.

Yang, D., W. Shao, P. Yeh, H. Yang, S. Kanae, and T. Oki (2009), Impact of vegetation coverage on regional water balance in the nonhumid regions of China, *Water Resour. Res.*, *45*, W00A14, doi:10.1029/2008WR006948.

Zhang, L., W. R. Dawes, and G. R. Walker (2001), Response of mean annual evapotranspiration to vegetation changes at catchment scale, *Water Resour. Res.*, *37*(2), 701–708.